

Effect of Laser Multiple Remelting on the Geometric Parameters and Component Distribution of CrMnFeCoNi High-Entropy Alloys Coatings Fabricated on Al Alloy by Laser Cladding

Chao Chen¹ · Xinyue Cong¹ · Jing Lv² · Baosong Guo¹ · Huijing Zhang¹

Received: 29 January 2023 / Accepted: 18 July 2024
© The Indian Institute of Metals - IIM 2024

Abstract In this work, CrMnFeCoNi high-entropy alloy coating was successfully prepared on the surface of aluminum alloy by laser cladding. The relationship between the geometrical morphology of the coating cross section and laser process parameters was systematically studied. The influence of line energy and the number of remelting on the morphology of the coating cross section was mainly discussed, and the uniformity of coating elements distribution was regulated by multiple remelting. The coating cross-sectional dimensions, element distribution and hardness values were measured by stereomicroscope, energy-dispersive spectrometer and microhardness tester. The results show that the cladding height of CrMnFeCoNi high-entropy alloy coating increases first and then decreases with the increase of line energy, but the value changes slightly. The cladding width and cladding depth gradually increase with the increase of line energy and remelting times. When the coating is remelted 2 times, there is an incompletely melted island-like CrMnFeCoNi high-entropy alloy powder in the upper left corner of the coating. When remelting 3 times, there is no incompletely melted high-entropy alloy aggregate, and the uniformity of coating is better than that when remelting 2 times. The uniformity of coating composition is the best after 4 remelts, and the hardness of coating reaches 459.67HV_{0.2} when the line energy is 0.67 J/mm for 4 remelts.

Keywords Laser cladding · High-entropy alloy · Laser multiple remelting · Geometric morphology · Component distribution

1 Introduction

Aluminum alloy has many advantages such as high specific strength, good electrical conductivity, good thermal conductivity and low density, and is widely used in automobile, ship, aerospace and other fields [1, 2]. However, the application range of aluminum alloy is limited due to its low hardness, wear resistance and poor corrosion resistance. Therefore, the service life of the material and its application range can be extended by surface modification technology to improve surface performance [3, 4]. Laser cladding technology is a process that uses a laser beam to melt the cladding material and the surface of the substrate, and after solidification to form a good metallurgical bond between them. Compared with aluminum alloy surface modification methods such as thermal spraying [5], anodizing [6] and electroplating [7], laser cladding has the advantages of high laser energy, fast heating and cooling speed, high quality of cladding layer and compatibility with the substrate. It has the benefits of metallurgical bonding and other advantages and has a strong application prospect in the surface modification of materials [8].

Wu et al. [9] successfully prepared Ni-based composite coatings on the surface of AlSi₇Mg aluminum alloy by laser cladding and explored the microstructure and wear properties of the coatings. The results show that the improvement of coating hardness and wear performance is mainly related to the formation and uniform distribution of the coating surface and middle structure. Jeyaprakash et al. [10] used the laser cladding method to prepare the H13 steel coating

✉ Huijing Zhang
zhanghuijing@nefu.edu.cn

¹ College of Mechanical and Electrical Engineering, Northeast Forestry University, No.26 Hexing Road, Harbin 150040, People's Republic of China

² Beijing Research Institute of Telemetry, No.1 Nandahongmen Road, Fengtai District, Beijing 10076, People's Republic of China

on the surface of AA6061 aluminum alloy. It was found that the structure of the coating is composed of carbides and martensite. Carbides are the main contributor to the increase in hardness and wear resistance of coatings. Liu et al. [11] prepared $\text{SiC}_p/\text{Al-Si}$ composite coating by laser cladding method on the surface of 4032 aluminum alloy. It was found that increasing the content of $\text{SiC}_p\text{-Cu}$ would improve the hardness and wear performance of the coating, which provided a new way for surface modification of aluminum alloy. Li et al. [12] prepared Ti/TiBCN composite coatings by laser cladding on the surface of 7075 aluminum alloy and found that the laser cladding process parameters had a high correlation coefficient with the geometry and size of the coating. Grohol et al. [13] used off-axis powder spraying laser cladding method to clad 6061 aluminum alloy powder on 6061-T6511 aluminum alloy substrate, and explored the relationship between coating geometry and processing parameters. When the laser power is 3625 W, the scanning speed is 2.5 mm/s, and the powder feeding speed is 0.18 g/s, the hardness of the coating and the heat-affected zone is the highest and the quality is good.

High-entropy alloy has high mixing entropy and is easy to form a simple solid solution structure, with high hardness, excellent wear resistance, corrosion resistance, fatigue resistance and high-temperature oxidation resistance. Therefore, many scholars have achieved the purpose of surface modification of materials by preparing high-entropy alloy coatings [14–16]. Nguyen et al. [17] prepared $\text{Al}_x\text{FeMnNiCrCu}_{0.5}$ high-entropy alloy coating on 1045 steel substrate by laser cladding. The results show that the coating phase transforms from a single FCC phase to a two-phase FCC/BCC phase, and then to a single BCC phase with the increase of Al content. Wang et al. [18] studied the effect of specific energy on the microstructure and properties of laser cladding FeCoCrNi high-entropy alloy coatings. Zhang et al. [19] prepared FeNiCoCrTi_{0.5} high-entropy alloy coatings with different process parameters on the surface of 45 steel, and found that the hardness of the coating was the highest and the wear resistance was the best when the specific energy was 72.22 J mm^{-2} .

However, due to the rapid heating and cooling characteristics of laser cladding, problems such as uneven distribution of cladding materials will occur in the coating. In order to improve the quality of the coating, Cai et al. [20] carried out multi-pass in situ laser remelting treatment on the (FeMnCrNiCo + 20%TiC) coating. The results show that the uniformity of the size and distribution of ceramic particles in the coating is greatly improved after remelting. Zhao et al.

[21] performed laser remelting on the surface of the nickel-based alloy coating and found that the surface roughness of the coating was reduced by more than $2 \mu\text{m}$ after remelting, and laser remelting could effectively improve the surface quality of the coating. In this paper, we plan to use laser cladding CrMnFeCoNi high-entropy alloy to improve the surface properties of 2A14 aluminum alloy. The uniformity of element distribution of coating is adjusted by multiple remelting to improve the quality of the coating. The optimal remelting process is explored, and the remelting regulation mechanism is clarified.

2 Materials and Methods

The substrate material in this experiment is a 2A14 aluminum alloy plate with a size of $100 \text{ mm} \times 100 \text{ mm} \times 10 \text{ mm}$, and its specific composition is shown in Table 1. The CrMnFeCoNi high-entropy alloy powder with a particle size of $15\text{--}53 \mu\text{m}$ and an equimolar ratio was used as the cladding material. Before the start of the experiment, the aluminum alloy base material was polished with sandpaper to remove the oxide film, rinsed with anhydrous ethanol and then dried with strong cold air with a hair dryer.

The method used in this experiment is the preset powder method with a preset powder thickness of $100 \mu\text{m}$. High-entropy alloy powders are evenly coated on the substrate by means of a horizontal scraper in the laser cladding equipment. Selective laser cladding of high-entropic alloy powders on the substrate surface was done by a laser beam. IPG YLR-500 fiber optic laser with a spot diameter of $70 \mu\text{m}$ was used. In order to obtain coatings with uniform element distribution and micron thickness, less line energy is required, so lower laser power and higher scanning speed are used in this experiment. In this experiment, the coating uniformity was controlled by multiple remelting, and the experimental parameters are shown in Table 2.

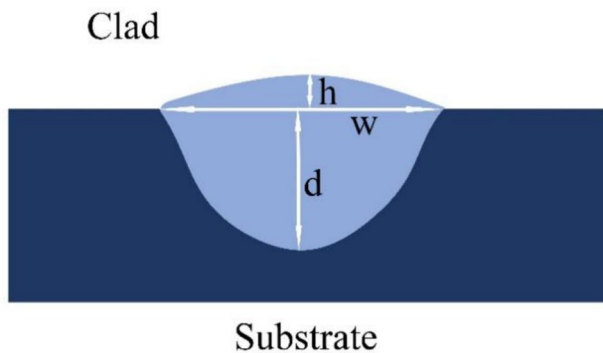
The coating cross section is obtained by wire electric discharge cutting technology. The size of the coating cross section mainly includes cladding height h , cladding depth d and cladding width w , as shown in Fig. 1. The cross section of the coating is etched with Keller reagent. The morphology is observed with a stereo microscope, and its size is measured. The composition distribution of elements in coatings was characterized by scanning electron microscopy (SEM) equipped with an energy-dispersive spectrometer (EDS). The microhardness tester was used to measure the coating Vickers hardness of the layer cross section.

Table 1 Chemical composition of 2A14 aluminum alloy substrate (wt.%)

Si	Cu	Mg	Zn	Mn	Ti	Ni	Fe	Al
0.6	4.3	0.6	0.1	0.8	0.1	0.1	0.5	Bal.

Table 2 Experimental parameters of laser cladding

No	Power (W)	Speed (mm/s)	Line energy (J/mm)	Remelting times
1	200	100	2	2
2	200	100	2	3
3	200	100	2	4
4	200	200	1	2
5	200	200	1	3
6	200	200	1	4
7	200	300	0.67	2
8	200	300	0.67	3
9	200	300	0.67	4
10	200	400	0.5	2
11	200	400	0.5	3
12	200	400	0.5	4

**Fig.1** Sketch picture of geometric parameters of coating cross section

3 Results and Discussion

3.1 Geometric Parameters of Laser Cladding CrMnFeCoNi coating

Figure 2 shows the geometry of coating cross section with different line energy and 2, 3 and 4 remelting times, respectively. In this paper, the line energy is used to describe the influence law of the coating geometry [22]:

$$E = \frac{P}{v} \quad (1)$$

where P is laser power, v is scanning speed. Figure 2a, b, c, d shows the geometrical topography of the coating cross section with different remelting times when the line energy is 2 J/mm, 1 J/mm, 0.67 J/mm and 0.5 J/mm, respectively. It can be seen from the figure that under same line energies, the penetration depth of the coating cross section increases with the increase of the number of remelting times. The reason is that with the increase of remelting times, the heat

accumulation of the substrate also increases [23]. The temperature of the substrate increases continuously, while the temperature gradient of the substrate around the molten pool gradually decreases. The heat conduction from the molten pool to the substrate decreases, and the heat used to maintain the molten pool increases, so the cladding depth increases. At the same time, we can also see that when the number of remelting is the same, the cladding depth of the coating cross section decreases gradually with the decrease of the line energy. According to Eq. (1), the laser power is unchanged; the scanning speed is accelerated; the energy in the molten pool decreases per unit time; the interaction time between the laser beam, the cladding powder and the substrate becomes shorter; and the cladding depth gradually decreases. However, no obvious linear relationship was found between the cladding height and the cladding width with line energy or remelting times. In order to accurately obtain the variation law of the geometric parameters of the coating, the geometric dimensions of the cross section in Fig. 2 were measured, and the measurement results are shown in Fig. 3.

Figure 3a shows the effect of line energy on the cladding height when the number of remelting times is 2, 3 and 4. The measurement results show that the cladding heights are all in the range of 17–28 μm . With the increase of line energy, the cladding height shows a trend of first increasing and then decreasing. When the line energy is 1 J/mm, the cladding height is the highest. The reason is that the preset powder method is used in this experiment, and the powder thickness is constant. According to Eq. (1), the line energy increases with the decrease of the scanning speed, and the decrease of the scanning speed means that the time of the laser acting on the cladding powder increases, the laser energy increases, the size of the molten pool increases, and the cladding height becomes higher [24]. During the laser cladding process, the cooling rate of the coating is fast, and the surface tension acts on the coating in the molten state for a short time, so that the surface curvature is relatively gentle after the coating is solidified [20]. When the line energy is 0.5 J/mm and 0.67 J/mm, the cladding height of the coating increases with the increase of remelting times.

Figure 3b shows the relationship between line energy and cladding width under different remelting times. The cladding width is 306.81 μm when the line energy is 2 J/mm after 2 remelts, which is about 1.5 times of that when the line energy is 0.5 J/mm. When the line energy is 2 J/mm, remelting 2, 3 and 4 times, the cladding width of the coating cross section is 306.81 μm , 323.44 μm and 333.3 μm , respectively. With the increase of remelting times, the cladding width is 1.05 times and 1.03 times that of the previous cladding.

Figure 3c shows the relationship between line energy and cladding depth for different remelting times. The cladding depth increases with the increase of line energy and

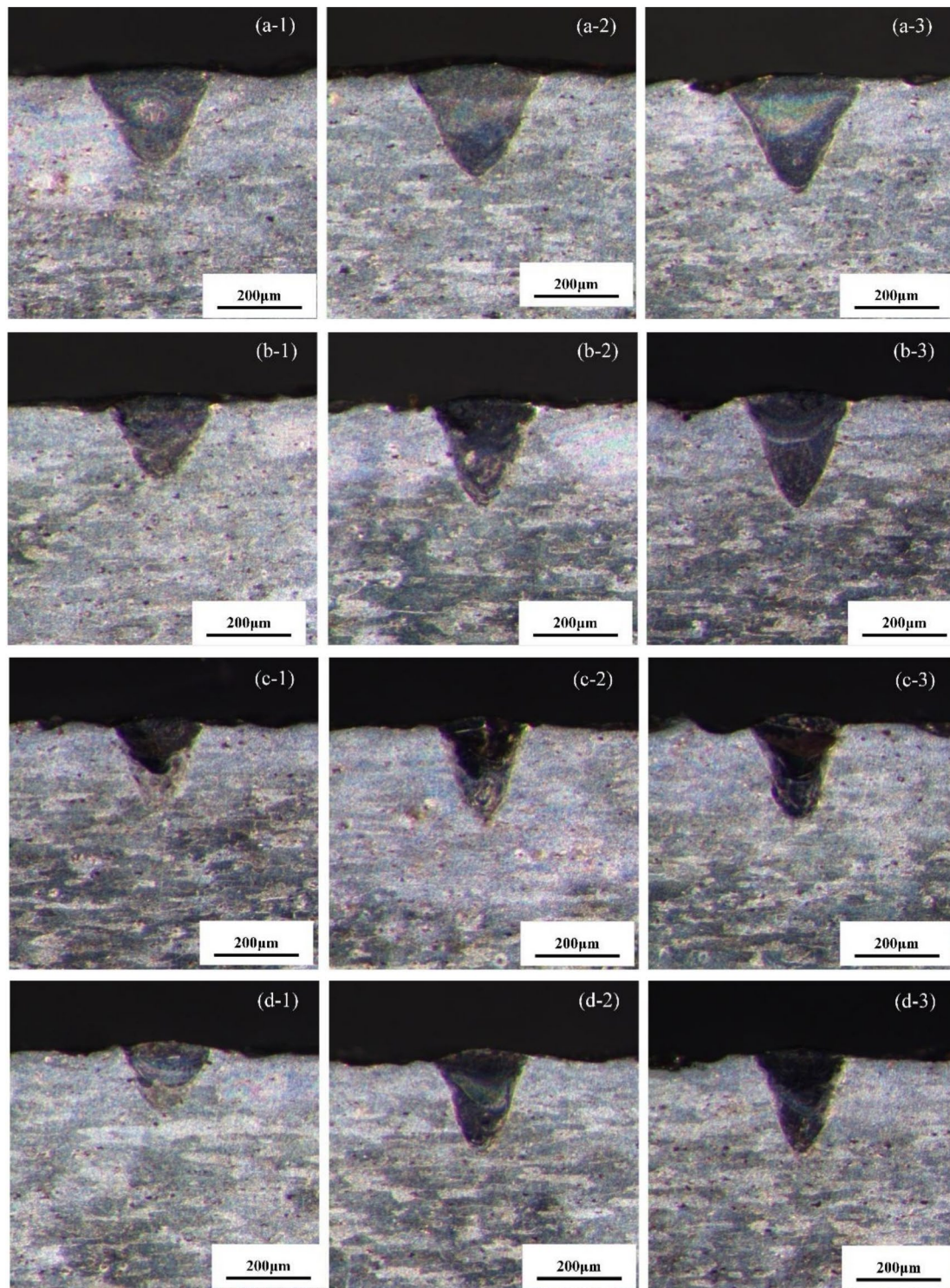


Fig. 2 Geometry of coating cross section with different line energy and 2, 3 and 4 remelting times, respectively. **a** The line energy is 2 J/mm, **b** 1 J/mm, **c** 0.67 J/mm and **d** 0.5 J/mm

remelting times. The cladding depth was 215.64 μm when the line energy was 2 J/mm after 2 remelting, which was 1.35 times of the cladding depth when the line energy was

0.5 J/mm. When the line energy is 2 J/mm, remelting 2, 3 and 4 times, the penetration depth of the coating cross section is 215.64 μm , 247.66 μm and 271.7 μm , respectively.

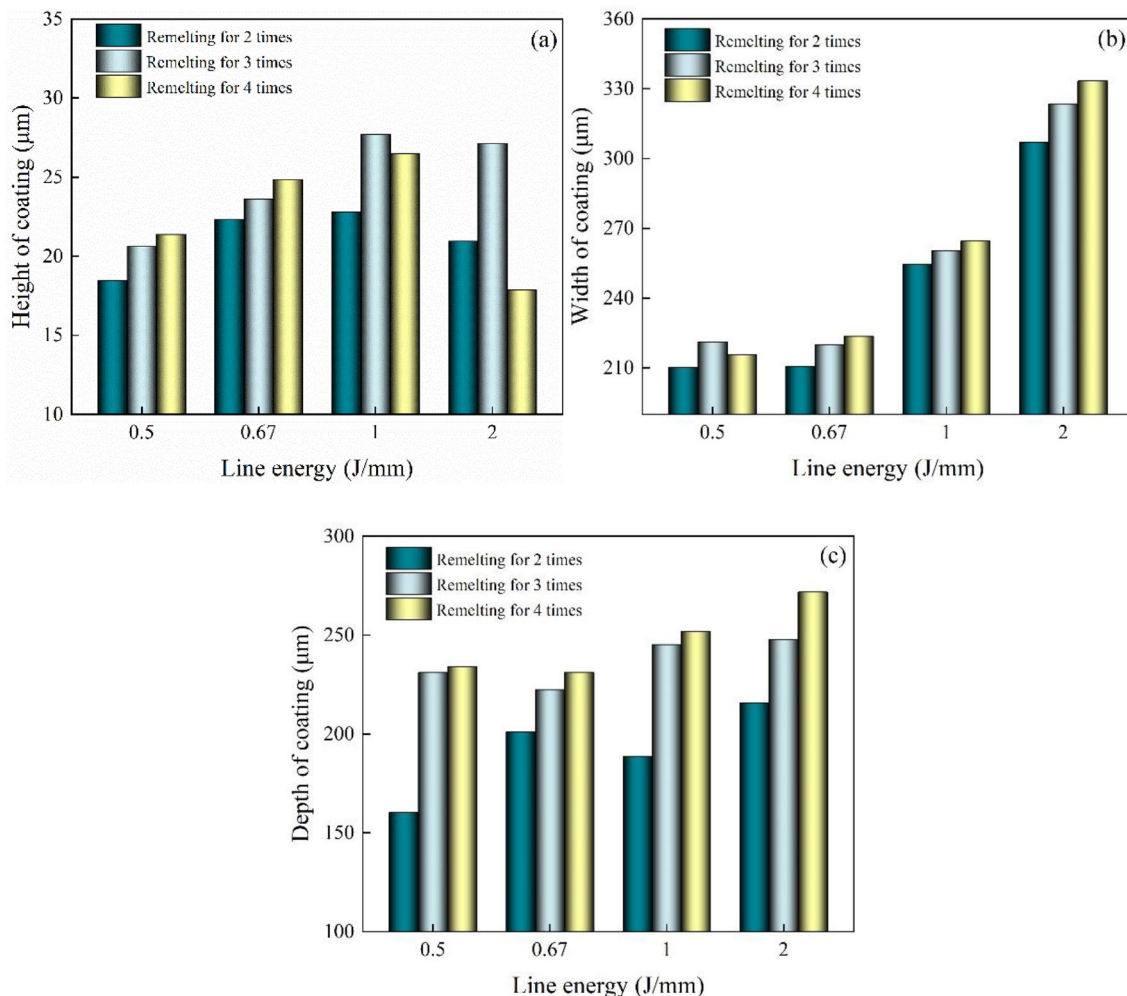


Fig. 3 Relationship between line energy and cladding height (a), cladding width (b) and cladding depth (c) under different laser cladding process parameters

With the increase of remelting times, the cladding depth is 1.15 times and 1.1 times that of the previous cladding.

3.2 Element Distribution of Laser Cladding CrMnFeCoNi Coating

In order to explore the relationship between the number of remelting and the uniformity of element distribution in the coating, the cross section of the coating with 1 J/mm line energy and 2, 3 and 4 times of remelting is scanned and the composition distribution is observed. The results are shown in Fig. 4, where the brighter colors and larger values in the legend indicate higher elemental content. As shown in Fig. 4a, there is an “island” patch in the upper left corner of the coating. The analysis shows that the “island” patch is a CrMnFeCoNi high-entropy alloy powder that has not been completely melted. There are several small highlights in Fig. 4b where there is a clear light–dark boundary between

the upper part of the coating and the lower part of the coating. Figure 4c shows the distribution of coating elements which have been remelted 4 times, which is further reduced and smaller than the number of highlights in Fig. 4b. No obvious light–dark boundary appears in the coating, indicating that the composition of high-entropy alloy coating is more uniform. It can be seen that with the increase of the number of remelting, the cladding area of the coating gradually increases and the uniformity of the coating becomes better and better.

Table 3 describes the EDS results of coatings with different remelting times at line energy of 1 J/mm. It can be seen that the weight fraction of high-entropic alloy elements increases with the number of remelts. This is because the preset powder method is used in this experiment, and the remelting is carried out immediately after laser cladding. With multiple remelting, the non-melted high-entropic alloy powder on the surface of aluminum substrate will be further

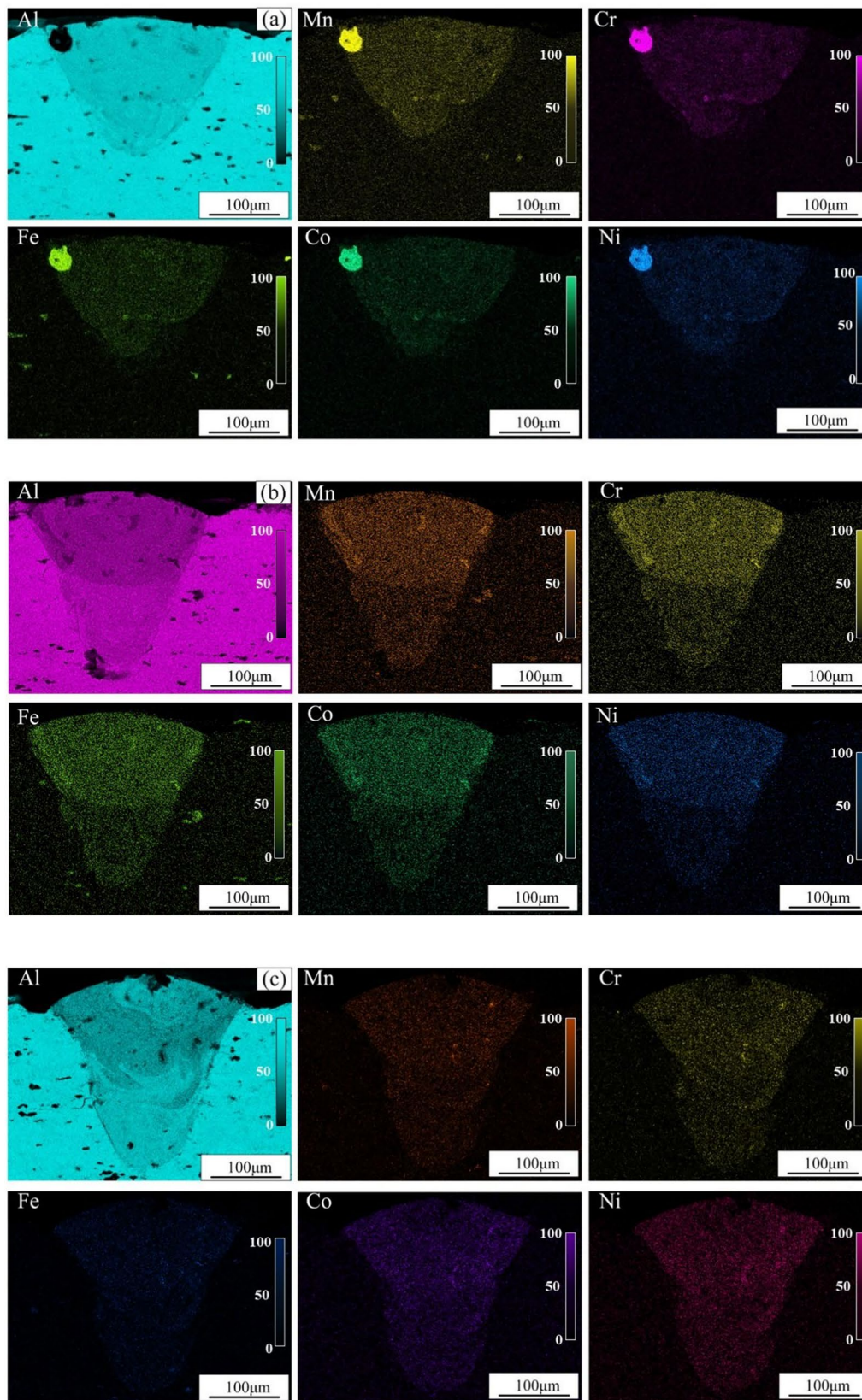


Fig. 4 EDS characterization of coating cross section with different remelting numbers at 1 J/mm line energy. **a** Remelting 2 times, **b** remelting 3 times and **c** remelting 4 times (color figure online)

Table 3 EDS results (wt.%) of coatings with different remelting times at line energy of 1 J/mm

Sample	Al	Cu	Mn	Ni	Co	Fe	Cr
Remelting 2 times	90.96	5.35	1.16	0.63	0.61	0.7	0.60
Remelting 3 times	89.00	5.21	1.56	1.09	1.05	1.13	0.96
Remelting 4 times	85.26	8.10	1.60	1.51	1.27	1.24	1.02

melted into the molten pool. As a result, the weight fraction of high-entropic alloys increases, which in turn improves the coating quality.

Figure 5 shows the schematic diagram of atomic diffusion under different remelting times. The atomic concentrations of Cr, Mn, Fe, Co and Ni in the cladding powder are higher than those in the aluminum alloy substrate. There is a concentration gradient as shown in Fig. 4; the distinct light and dark zones indicate different element contents. It is very easy to diffuse under the action of heat, from the coating with high concentration to the substrate, while the Al atom in the substrate diffuses from the substrate to the coating. This process follows Fick's first law [25]. Figure 5b shows that a high-entropy alloy aggregate in the upper left corner of the coating in the secondary remelting area. This is because temperature affects the diffusion rate. Argon and substrates accelerate the cooling of the molten pool. Therefore, the partially melted high-entropic alloy solidifies before full diffusion, resulting in poor uniformity of the upper half of the coating and easy aggregation. The coating material is not uniformly distributed after 2 remelts. When

remelted 3 times, the Al atoms in the substrate and Cr, Mn, Fe, Co and Ni atoms in the coating can interdiffuse for more time, and the aggregates disappear. However, there is a clear light–dark boundary between the upper and lower part of the coating in the EDS characterization, indicating that there is still a concentration gradient at this time. When remelted 4 times, further diffusion of atoms results in a decrease in the concentration gradient, which improves the uniformity of the coating.

3.3 Hardness

The hardness measurement was performed at the upper middle part of the coating cross section, where the elements are more uniformly distributed, by hitting points at equal intervals laterally. The highest coating hardness of 459.67HV_{0.2} was achieved when the line energy was 0.67 J/mm and remelted 4 times. For CrMnFeCoNi high-entropy alloy, the addition of sufficient amount of Al to this high-entropy alloy will lead to lattice expansion and thus solid solution strengthening of CrMnFeCoNi

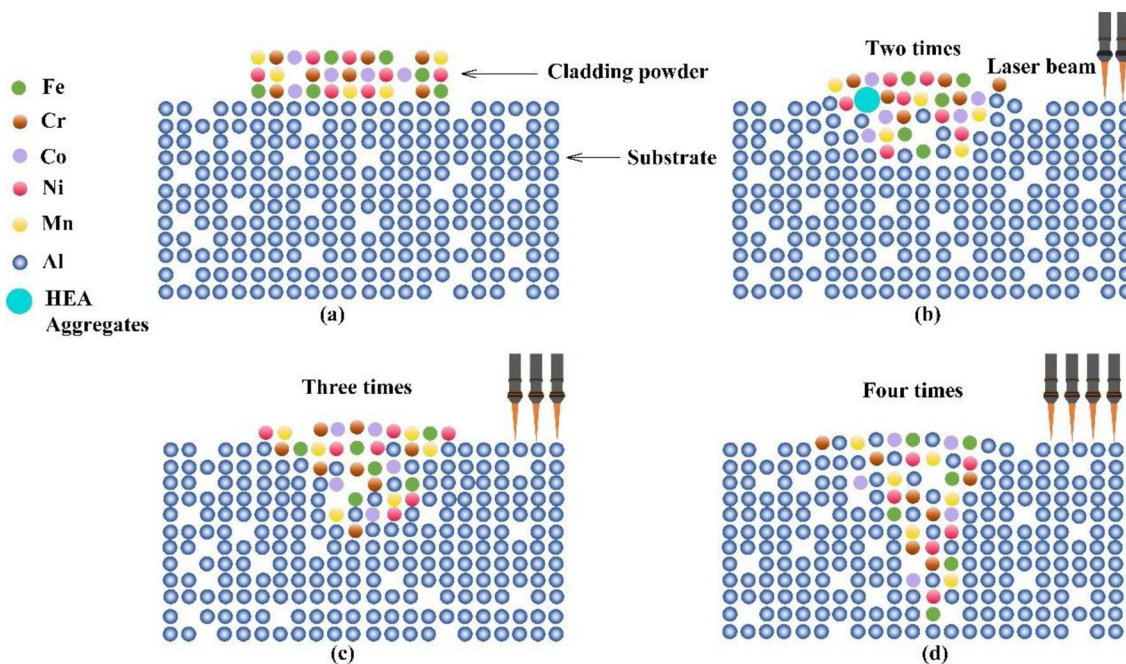


Fig. 5 Schematic diagram of element diffusion under different remelting times. **a** Before laser cladding, **b** remelting 2 times, **c** remelting 3 times and **d** remelting 4 times

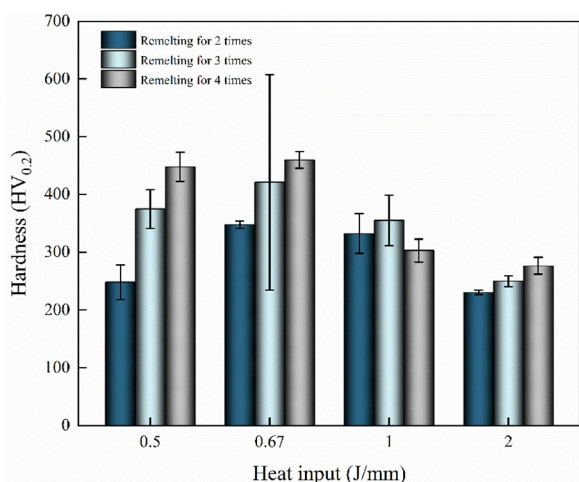


Fig. 6 Relationship between line energy and coating hardness

high-entropy alloy due to the relatively large atomic radius of Al. This will change the high-entropy alloy from FCC structure to BCC structure, which will result in an increase in the hardness of this high-entropy alloy [26]. The hardness results in this paper are similar to this conclusion. Figure 6 shows that the hardness increases and then decreases as the line energy increases. The reason why the hardness rises first is that as the line energy increases, the aluminum element in the substrate is gradually diluted into the CrMnFeCoNi high-entropy alloy coating, and Al can easily form hard intermetallic phases with Ni, Fe and Co in the coating, which leads to a significant increase in the hardness of the coating. The subsequent decrease in hardness is due to a further increase in the line energy, which leads to a significant dilution of the high-entropy alloy coating by the aluminum alloy substrate, so the hardness decreases slightly. At the same time, it can also be seen from the figure, with the increase of remelting times, the coating hardness gradually increased. With the line energy of 0.5 J/mm, remelting times of 2, 3 and 4, the hardness of the coating was 248.43HV_{0.2}, 374.77HV_{0.2} and 447.77HV_{0.2}, respectively. Among them, the hardness of remelting 3 times increased by 51% compared to remelting 2 times, and the hardness of remelting 4 times increased by 19% compared to remelting 3 times. This is mainly due to the comprehensive effect of fine grain strengthening and solid solution strengthening caused by laser remelting. Laser remelting cooling rate is fast, so as to improve the nucleation rate and inhibit the grain growth, so as to achieve fine grain strengthening. Grain refinement can form a large number of grain boundaries, which can effectively hinder the movement of dislocations, thereby improving the strength and hardness of materials; on the other hand, the atomic radius of Al is relatively large, and

laser remelting will melt enough Al into the high-entropy alloy coating, resulting in lattice distortion. Lattice distortion will increase the resistance of dislocation movement, making it difficult for the crystal to slip, thus further improving the hardness of the coating.

4 Conclusions

CrMnFeCoNi high-entropy alloy coating was successfully prepared on 2A14 aluminum alloy surface by laser cladding, and the element distribution of the coating was evenly distributed by laser remelting for many times. Geometric morphology, element distribution and mechanical properties of the laser clad coating remelted several times were examined by stereo microscope, EDS and microhardness. The important findings of this study are:

1. The cladding depth and width increase with the increase of line energy and number of remelting. When the line energy is 2 J/mm, with the increase of remelting times, the cladding width is 1.05 times and 1.03 times of the previous cladding, and the cladding depth is 1.15 times and 1.1 times of the previous cladding, respectively. The cladding height ranged from 17 to 28 μm , reaching the level of micron coating.
2. When the number of remelting reaches 4 times, the atoms in the cladding material and the substrate further diffuse with each other, thus further homogenizing the coating composition.
3. With the increase of line energy, the hardness of the coating first increases and then decreases. When the line energy is 0.67 J/mm and remelted 4 times, the hardness of the coating reaches 459.67HV_{0.2}.

Authors Contributions Not applicable.

Funding No funding.

Data Availability Not applicable.

Declarations

Conflict of interest No conflict of interest exists in the submission of this manuscript, and the manuscript is approved by all authors for publication.

Ethical Approval Not applicable.

Consent to Participate Not applicable.

Consent for Publication Not applicable.

References

1. Chi Y, Gu G, Yu H, and Chen C, *Optics and Lasers in Engineering* **100** (2018) 23.
2. Quazi M M, Fazal M A, Haseeb A S M A, Yusof F, Masjuki H H, and Arslan A, *Critical Reviews in Solid State and Materials Sciences* **41** (2016) 106.
3. D'amato C, Betts J C, and Buhagiar J, *Surface & Coatings Technology* **244** (2014) 194.
4. Zhang J, Song B, Wei Q, Bourell D, and Shi Y, *Journal of Materials Science & Technology* **35** (2019) 270.
5. Bao Y, Gawne D T, Gao J, Zhang T, Cuenca B D, and Alberdi A, *Surface & Coatings Technology* **232** (2013) 150.
6. Lu J, Wei G, Yu Y, Guo C, and Jiang L, *Surfaces and Interfaces* **13** (2018) 46.
7. Prasad D S, Ebenezer N S, and Shoba C, *Transactions of the Indian Institute of Metals* **70** (2017) 2601.
8. Shu F, Yang B, Dong S, Zhao H, Xu B, Xu F, Liu B, He P, and Feng J, *Applied Surface Science* **450** (2018) 538.
9. Wu X Q, Yan H, Xin Y, Yu B, Hu Z, and Sun Y, *Rare Metal Materials and Engineering* **49** (2020) 2574.
10. Jeyaprakash N, Yang C H, and Sivasankaran S, *Transactions of the Indian Institute of Metals* **73** (2020) 1611.
11. Liu Y, Li G D, and Jiang W T, *Materials* **12** (2019) 1537.
12. Li Y X, Zhang P F, Bai P K, Zhao Z-Y, and Liu B, *Materials* **11** (2018) 1551.
13. Grohol C M, Shin Y C, and Frank A, *Surface and Coatings Technology* **415** (2021) 127099.
14. Miracle D B, and Senkov O N, *Acta Materialia* **122** (2017) 448.
15. Pickering E J, and Jones N G, *International Materials Reviews* **61** (2016) 183.
16. Zhang Y, Zuo T T, Tang Z, Gao M C, Dahmen K A, Liaw P K, and Lu Z P, *Progress in Materials Science* **61** (2014) 1.
17. Nguyen T, Ly X, Huang M, Qin Y, and Yang S, *Journal of Thermal Spray Technology* **31** (2022) 980.
18. Wang L L, Gao Z N, Wu M Y, Weng F, Liu T, and Zhan X, *Metals* **10** (2020) 1464.
19. Zhang Y, Han T F, Xiao M, and Shen Y, *International Journal of Minerals Metallurgy and Materials* **27** (2020) 630.
20. Cai Y, Cui Y, Zhu L, Tian R, Geng K, Li H, and Han J, *Surface Engineering* **37** (2021) 1496.
21. Zhao Y Z, Sun J, Guo K, and Li J, *Journal of Laser Applications* **31** (2019) 1.
22. Chen Z J, Liu Y, Wu H, Zhang W, Guo W, Tang H, and Liu N, *Applied Surface Science* **357** (2015) 2347.
23. Feng Q N, Tian Z J, and Liang H X, *Applied Laser* **37** (2017) 51.
24. Chen G X, Zeng X Y, and Wang Z M, *Machine Tool & Hydraulics* **38** (2010) 1.
25. Hu G X, Cai X, and Rong Y H, in *Fundamentals of Materials Science*, Shanghai Jiao Tong University Press, (2010).
26. Xian X, Zhong Z H, Lin L J, Zhu Z X, Chen C, Wu Y C, et al., *Rare Metals* **41** (2018) 1015.

Publisher's Note Springer Nature remains neutral with regard to jurisdictional claims in published maps and institutional affiliations.

Springer Nature or its licensor (e.g. a society or other partner) holds exclusive rights to this article under a publishing agreement with the author(s) or other rightsholder(s); author self-archiving of the accepted manuscript version of this article is solely governed by the terms of such publishing agreement and applicable law.